ASSESSMENT OF AIR CHANGE EFFECTIVENESS AND THERMAL COMFORT IN A NATURALLY VENTILATED KITCHEN WITH INSECT-PROOF SCREEN USING CFD

Jayasree T K,[1] Jinshah B S,[2] Lakshmi Visakha V,[1] and Srinivas Tadepalli[1]

ABSTRACT

Many dwellings in warm-humid climates attain a comfortable environment by natural ventilation. The opening of exterior windows for ventilation allows the entry of insects along with the breeze. As a remedy, occupants install insect-proof screens on windows resulting in reduced airflow into the interior. This study attempts to evaluate the air change effectiveness and thermal comfort in a residential kitchen with insect-proof screens. A kitchen with insect-proof screens on the windows is compared with a case without insect-proof screens. Numerical simulation was conducted using ANSYS Fluent 2019 R2. The insect-proof screen is modelled as a porous media. The air velocity and temperature measurements were validated by measurements in a real scenario. The presence of insect-proof screens reduced the air velocity inside the space by 82%. However, the airflow pattern in the case with screens was more uniformly distributed. The mean age of the air was considerably higher in the case with insect-proof screens, which in turn resulted in a reduced ACE. The presence of an insect-proof screen resulted in a Predicted Mean Vote (PMV) of 2.79 indicating a 'hot' sensation, whereas in the other case, the comfort vote is only 1.93 indicating a 'warm' sensation. The presence of insect-proof screens on windows reduced the air velocity and ventilation efficiency, contributing to increased thermal discomfort in the kitchen.

KEYWORDS

thermal comfort, air change effectiveness, insect-proof screen, kitchen, computational fluid dynamics, age of air

INTRODUCTION

Natural ventilation is a prominent passive strategy adopted by dwellings in warm-humid climates to achieve a comfortable indoor environment (Haase & Amato, 2009; Indraganti, 2010). Cross ventilation is ensured by opening exterior windows to allow fresh air flow into the buildings. This helps to attain better indoor air quality and ventilation, which are important parameters in assessing buildings for sustainability concepts or any green ratings. Green rating systems like LEED and GRIHA promote naturally ventilated buildings to achieve energy efficiency

1. Department of Architecture, National Institute of Technology, Tiruchirappalli, India
2. Department of Mechanical Engineering, National Institute of Technology, Tiruchirappalli, India

and better indoor air quality. Thermal comfort is a major concern for indoor air quality, and it can affect the occupant performance (Al Horr et al., 2016; Tarantini et al., 2017) and energy consumption in residential buildings (Kwok et al., 2017). As a key component in sustainable design, the potential of natural ventilation in achieving thermal comfort (Ge et al., 2019; Q. Zhang & Yu Lau, 2017) and reducing energy consumption (Tong et al., 2016) is assessed in various cities with warm-humid climates. However, the opening of exterior windows and doors for natural ventilation enhances the entry of insects and flies into the interior, along with the natural breeze (Snehalatha et al., 2003). Insect-proof screens are widely used in places which are prone to mosquitoes and flies due to health concerns related to artificial pesticides and insect repellents. It has become a common practice to install insect-proof screens on operable windows to prevent the entry of insects without compromising natural ventilation completely.

The effect of insect-proof screens on airflow and ventilation is investigated by theoretical studies, experiments and numerical approaches. The theoretical approaches for the characterization of airflow through screens includes Bernoulli's equation (Muñoz et al., 1999) and the Forchheimer equation (Miguel et al., 1997). Experimental studies for analysing flow through screens were conducted by Miguel (1998), and wind tunnel experiments were carried out by López, Molina-Aiz, Valera, & Peña (2016). Research based on numerical approaches (Bartzanas et al., 2002; Cohen, 2015; Fatnassi et al., 2006; Teitel, 2010) was conducted by using various commercially available software for computational fluid dynamics (CFD). Few studies validated the CFD results with the data obtained with wind tunnel experiments (Ravikumar & Prakash, 2011; Valera et al., 2006). Emerging methods for investigating the flow characteristics through screens involve CFD simulations and its validation by Particle Image Velocimetry (PIV) (Santolini et al., 2019).

CFD has played a prominent role in assessing and creating spaces for appropriate ventilation. The use of CFD for indoor airflow prediction has been validated in many studies (Hawendi et al., 2019; Horikiri et al., 2014; Sarkar & Bardhan, 2018). The accuracy of the simulation depends on several factors and selection of the appropriate turbulence modelling approach has been identified as a vital issue. Nielsen (2015) discussed the selection of appropriate governing equations, turbulence models, and addressing the situations where several steady-state solutions may take place. All turbulent models have varied capabilities, and it is challenging to decide on a single model that can predict all the flow elements in an optimized form. Franke et al. (2004) discussed several recommendations for the use of CFD modelling in wind engineering.

Modelling of insect-proof screens for CFD analysis is done predominantly by modelling a porous slab. Teitel (2010) compared the results of simulation with porous slab and a realistic screen and achieved a good correlation with the pressure drops. Porous media modelling reduced computational time considerably. Bartzanas et al. (2002) studied the influence of an insect-proof screen in a tunnel greenhouse and identified that a screen reduces the airflow rate by 50% and increases the temperature inside the space. Airflow and temperature distribution were also affected by the wind direction. The reduction in ventilation rate is expected to affect the thermal comfort and Indoor Air Quality (IAQ) inside a space as it is established that natural ventilation improves thermal comfort and Indoor Air Quality (IAQ) using outdoor airflow (Persily, 2015).

Most of the studies on airflow through screens are conducted in the field of agricultural engineering (Fatnassi et al., 2006; López et al., 2016; Santolini et al., 2019) as investigations about the effect of insect-proof screens on the greenhouse climate and its impact on crop efficiency. Insect proof screens on window cavities in residences are evaluated in a few studies (Cohen, 2015; Ravikumar & Prakash, 2011; Vijayalaxmi & Sekar, 2010) and the spaces

considered in these studies do not resemble the characteristics associated with residential spaces. The presence of furniture or any other features inside the space has an influence on the airflow characteristics (Horikiri et al., 2015; Hormigos-Jimenez et al., 2018; Sabie & Ghiaus, 2019) and previous studies on habitable spaces with insect-proof screens (Cohen, 2015; Ravikumar & Prakash, 2011; Vijayalaxmi & Sekar, 2010) lack this consideration.

Green building standards like GRIHA in India require that naturally ventilated buildings comply with the ASHRAE standard 62.2 (2013) to achieve acceptable indoor air quality. The standard prescribes the need for local exhaust in specific areas like kitchens and bathrooms. The local exhaust can be a demand-controlled mechanical exhaust system (e.g., exhaust fans operated when needed) or a continuous mechanical exhaust system. However, it is observed that many residences do not follow these requirements for various reasons.

Residences in a warm-humid climate install insect-proof screens on windows and depend primarily on natural ventilation for thermal comfort even though warm discomfort is experienced in general. The kitchen space is observed to be warmer than other spaces because of the heat accumulation from cooking activities. The presence of exhaust fans or hoods are not common and depends on what families can afford, whereas the activities inside a kitchen are unavoidable and irrespective of seasons or comfort status. In this context, this study attempts to analyse the airflow characteristics, air change effectiveness and thermal comfort in a residential kitchen which has insect-proof screens fitted on the windows with computational fluid dynamics. The study considered a typical domestic kitchen with appliances and a granite slab to approximate the real scenario of the kitchen environment.

SCOPE OF THE STUDY AND GOVERNING EQUATIONS

Insect proof screens are gaining popularity on the operable windows of residences (Cohen, 2015; Norris & Collins, 2008; Ravikumar & Prakash, 2011; Vijayalaxmi & Sekar, 2010) to obstruct the entry of insects while allowing fresh air circulation inside the spaces. However, many studies have identified that the introduction of an insect-proof screen reduces the airflow rate and increases the temperature inside the space (Bartzanas et al., 2002; Ravikumar & Prakash, 2011; Vijayalaxmi & Sekar, 2010). A strong correlation between thermal comfort perception and wind sensation (Cândido et al., 2011; Feriadi & Wong, 2004; Wong et al., 2002) is also observed in previous studies. The presence of screens also affects the effectiveness of ventilation inside an area. A higher ventilation rate is preferred in the kitchen space of a naturally ventilated residence. Investigations on the state of air and flow characteristics (Chen et al., 2020; Debnath et al., 2016b, 2016a) and thermal comfort (Ravindra et al., 2019) inside a kitchen are conducted with open windows. However, the presence of insect-proof screens on the windows are expected to influence the flow characteristics and thermal environment inside the space. This investigation attempts to evaluate the role of the insect-proof screen on the air change effectiveness and thermal comfort in a space by numerical methods in CFD.

The basic conservation equations of mass, momentum and energy for fluid flow and are given below as equations (1) to (5):

$$\frac{\partial \rho}{\partial t} + \nabla \cdot (\rho \boldsymbol{U}) = 0 \tag{1}$$

$$\frac{\partial (\rho \boldsymbol{U})}{\partial t} + \nabla \cdot (\rho \boldsymbol{U} \otimes \boldsymbol{U}) = -\nabla p + \nabla \cdot \tau + S_M \tag{2}$$

Where the stress tensor, τ is related to the strain rate by:

$$\tau = \mu\left(\nabla \boldsymbol{U} + (\nabla \boldsymbol{U})^T - \frac{2}{3}\delta\nabla \cdot \boldsymbol{U}\right) \tag{3}$$

$$\frac{\partial\left(\rho h_{tot}\right)}{\partial t} - \frac{\partial p}{\partial t} + \nabla \cdot \left(\rho \boldsymbol{U} h_{tot}\right) = \nabla \cdot (\lambda \nabla T) + \nabla \cdot (\boldsymbol{U} \cdot \tau) + \boldsymbol{U} \cdot S_M + S_E \tag{4}$$

Where h_{tot} is the total enthalpy, related to the static enthalpy $h(T, p)$ by:

$$h_{tot} = h + \frac{1}{2}\boldsymbol{U}^2 \tag{5}$$

The term $\nabla \cdot (\boldsymbol{U} \cdot \tau)$ represents the work due to viscous stresses, and the term $\boldsymbol{U} \cdot S_M$ describes the work due to external momentum sources.

The concept of porous media is used to model the flow through insect-proof screens. This model retains both advection and diffusion terms. The equations for conservation of mass and momentum for a porous media are given below in equations (6) and (7):

$$\frac{\partial}{\partial t}\gamma\rho + \nabla \cdot \left(\rho K \cdot \boldsymbol{U}\right) = 0 \tag{6}$$

$$\frac{\partial}{\partial t}(\gamma\rho\boldsymbol{U}) - \nabla \cdot \left(\mu_e K\left(\nabla \boldsymbol{U} + (\nabla \boldsymbol{U})^T - \frac{2}{3}\delta\nabla \cdot \boldsymbol{U}\right)\right) + \nabla \cdot \left(\rho(K \cdot \boldsymbol{U}) \otimes \boldsymbol{U}\right) = \gamma S_M - \gamma\nabla p \tag{7}$$

Where $\boldsymbol{U}$ is the true velocity, γ is the volume porosity, μ_e is the effective viscosity, and S_M is a momentum source.

The fundamental law relating velocity and pressure drop in fluid flow through a porous media is Darcy's law expressed as equations (8) and (9):

$$\frac{\Delta p}{\Delta x} = -\frac{\mu}{K}u \tag{8}$$

$$\beta = \frac{Y}{K^{0.5}} \tag{9}$$

where μ is the fluid dynamic viscosity (*PaS*), K is the permeability to the fluid (m^2) of the media, ρ is the air density and β is the non-Darcy coefficient ($1/m$), and u is the fluid velocity.

However, Darcy's law defines the flow in porous media for low-velocity flows, which have a Reynolds number (R_e) lesser than 100 (Hellström & Lundström, 2006). There is a discrepancy in the experimental and Darcy's law results when the velocity magnitude and Reynolds number is increased. This difference is explained by Forchheimer by adding the effect of inertia to the equation by representing kinetic energy expressed as equation (10):

$$\frac{\partial P}{\partial x} = \frac{\mu}{K}u + \rho\left(\frac{Y}{K^{0.5}}\right)|u|u \tag{10}$$

Miguel et al. (1997) tested nine different thermal shading and insect screens by using physical models and defined the airflow characteristics in terms of permeability and porosity based on the Forchheimer equation. The inertial factor Y in porous screens differs from that for packed columns of spheres and is described by $Y = 4.36 \times 10^{-2}\epsilon^{-2.12}$ and insect screens have a permeability of less than 10^{-8} m^2.

Insect proof screens were considered as porous media initially by Miguel et al. (1997) in an experimental study to calculate pressure drop through insect-proof screens. It was established that for commonly observed situations (R_e < 100), the pressure drop through the porous screens could be expressed by the Forchheimer equation. This equation defines the airflow characteristics in terms of permeability and porosity. By testing several screens in the wind tunnel, the screen permeability (K) and inertial factor (Y) were correlated to porosity (γ) (Miguel, 1998) as:

$$K = 3.44\times10^{-9}\alpha^{1.6};\ Y = 4.3\times10^{-2}\gamma^{-2.13} \tag{11}$$

However, Valera et al. (2005) establish the pressure drop across a porous screen as a function of air velocity by testing with eleven different types of screen that led to a different correlation:

$$K = 5.68\times10^{-8}\alpha^{3.68};\ Y = 5.67\times10^{-2}\gamma^{-1.1604} \tag{12}$$

In both studies, pressure across the screen was plotted as a function of air velocity, and a second-order polynomial was fitted to the curve. The coefficients of the polynomial were then used to calculate the permeability and inertial factor. It is important to note that 14 screens with porosity ranging from 0.04 to 0.88 were tested to attain equation (11). This included both insect-proof and thermal screens. At the same time, equation (12) was obtained by experiments on woven micro-filament screen with porosity ranging from 0.288 to 0.483.

The case considered for this study is an existing typical residential kitchen having two windows on adjacent walls and a door on the third wall. The kitchen dimensions are 3m width, 3.9m depth and 3m height. The door is 0.8m X 2.0m, which is considered open in this study. The two windows of 1.2m X 1.2m are located at the centre of the walls with a sill height of 1.2m. Figure 1 (a) shows the schematic diagram of the case considered with open windows and door. The airflow direction is from west (-X to X axis) as described in Figure 1. A realistic scenario of the kitchen is replicated which includes a granite slab at the height of 0.80m, a single door refrigerator, and a gas stove with flame in one burner.

Assessment of ventilation effectiveness and thermal comfort

The reduction in air velocity and increase in interior temperature with insect-proof screens is expected to affect the ventilation efficiency and thermal comfort inside the space. Air Change Effectiveness (ACE) calculated from Mean Age of Air (MAA) is a measure to calculate the ventilation effectiveness of space, whereas, thermal comfort can be evaluated by a number of established thermal comfort indices.

FIGURE 1 (a) Plan of the kitchen (1-Stove flame, 2-Refrigerator, 3-Granite slab) (b) computational domain considered.

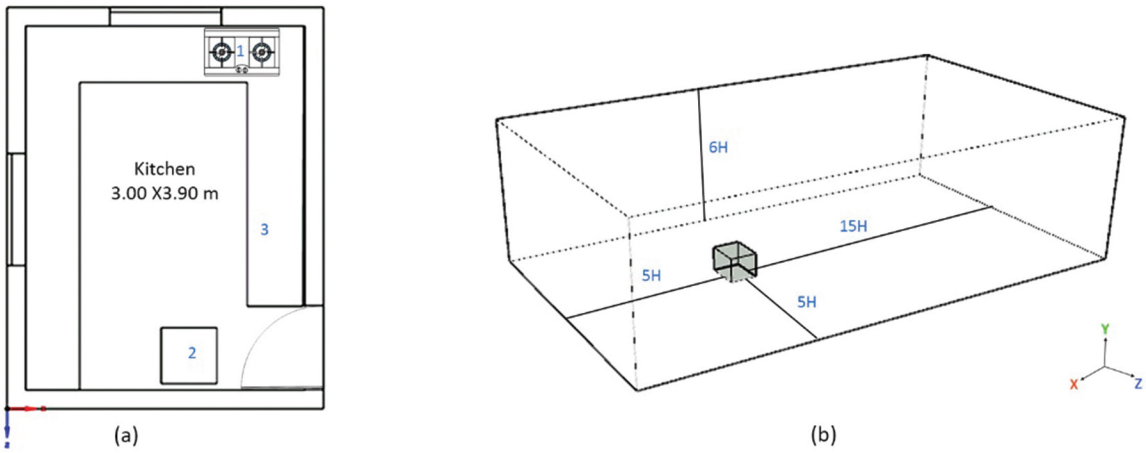

Mean Age of Air (MAA) and Air Change Effectiveness (ACE)

A measure of evaluating the ventilation efficiency in replacing the old air with the fresh air inside space is Air Change Effectiveness (ACE). It relates the Mean Age of Air (MAA) in a region with the nominal time constant of the ventilation. The mean age of air (expressed in seconds) in a room is defined as the average time elapsed since it reached various points in that particular space. The distribution of MAA in an area reflects the airflow pattern in a space. The age of air is an essential factor in assessing the quality of ventilation inside a space. The air change effectiveness (ACE) could be defined as the age of air that would be prevailing throughout the space if the air was perfectly mixed, divided by the average age of air within the breathing height. The local Air Change Effectiveness values are calculated with the equations (13) and (14) (Cehlin et al., 2018) at the level of 1.10m from the floor level.

$$\mathrm{ACE} = \frac{\tau_{nom}}{A_{avg}} \tag{13}$$

$$\tau_{nom} = \frac{V}{q} \tag{14}$$

where V (m^3) is the room air volume, q (m^3/s) is the inlet air flow rate, A_{avg} is the local mean age of air and τ_{nom} is the nominal time constant.

Thermal comfort

Fanger's comfort equations (Fanger, 1970) are used to calculate the thermal comfort index—Predicted Mean Vote (PMV). These comfort equations express the thermal balance of a human body, and this can be considered as an index equivalent to the thermal sensation vote by a group of people expressed on a seven-point scale as given in Table 2. ASHRAE standard 55:2017 prescribes that a comfort vote between +0.5 and –0.5 as the most comfortable and accepted by 90% of the occupants.

TABLE 1. Interpretation of comfort votes.

Comfort vote	Thermal sensation
+3	Hot
+2	Warm
+1	Slightly warm
0	Neutral
-1	Slightly cool
-2	Cool
-3	Cold

Predicted Mean Vote (PMV) can be estimated with the following mathematical expressions:

$$PMV = \left[0.303e^{(-0.036M)} + 0.028\right]L_{th} \tag{15}$$

Where,

$$L_{th} = \begin{Bmatrix} (M-W) - 3.05\times10^{-3}\left[5733 - 6.99(M-W) - p_a\right] - 0.42\left[(M-W) - 58.15\right] - 1.7\times10^{-5}M\left(5867 - p_a\right) \\ - 0.0014M\left(34 - t_a\right) - 3.96\times10^{-8}f_{cl}\left[(t_{cl}+273)^4 - (t_r+273)^4\right] - f_{cl}h_c\left(t_{cl} - t_a\right) \end{Bmatrix} \tag{16}$$

$$t_{cl} = 35.7 - 0.028\,(M-W) - I_{cl}\left\{3.96\times10^{-8}\ f_{cl}\left[\left(t_{cl}+273\right)^4 - \left(\overline{t_r}+273\right)^4\right] + f_{cl}h_c\left(t_{cl} - t_a\right)\right\} \tag{17}$$

$$h_c = \begin{cases} 2.38\left|t_{cl} - t_a\right|^{0.25} & \text{for } 2.38\left|t_{cl} - t_a\right|^{0.25} > 12.1\sqrt{v_{ar}} \\ 12.1\sqrt{v_{ar}} & \text{for } 2.38\left|t_{cl} - t_a\right|^{0.25} < 12.1\sqrt{v_{ar}} \end{cases} \tag{18}$$

$$f_{cl} = \begin{cases} 1.00 + 1.290I_{cl} & \text{for } I_{cl} \le 0.078 \text{ m}^2\text{K/W} \\ 1.05 + 0.645I_{cl} & \text{for } I_{cl} > 0.078 \text{ m}^2\text{K/W} \end{cases} \tag{19}$$

Where, I_{cl} is clothing insulation (m^2K/W), M is metabolic rate (W/m^2), W is Effective mechanical power (W/m^2), f_{cl} is clothing surface area factor, p_a is water vapour partial pressure (Pa), t_a is air temperature (^0C), t_{cl} is clothing surface temperature (^0C), t_r is mean radiant temperature, and (^0C), v_{ar} is relative air velocity (m/s).

The PMV model is incorporated into numerical simulation programs (Angelopoulos et al., 2017; Hawendi et al., 2019; Karacavus & Aydin, 2018) to assess comfort conditions. The PMV model considers still air conditions (0.1 m/s) whereas many studies have established that a higher

air movement can provide a cooling effect at the same temperature and humidity (Cândido et al., 2010; Loveday et al., 2016; Manu et al., 2014). ASHRAE standard 55-2013 proposed the calculation of PMV by considering the cooling effect provided by the air movement when the air velocity is observed to be higher than 0.2m/s. The Standard Effective Temperature (SET) model is used to account for the cooling effect of the airspeeds when the airspeed is greater than the maximum allowed in graphic comfort zone model.

METHODOLOGY

The study involved numerical simulations for predicting the air velocity, temperature, Mean Age of Air (MAA), Air Change Effectiveness (ACE) and Predicted Mean Vote (PMV). The air velocity predictions are validated by actual measurements obtained with an experimental setup in kitchens with and without insect-proof screens. Thermal comfort assessments were validated by comparing the PMV values obtained by simulation with the PMV output provide by the CBE Thermal comfort tool, which was developed according to ASHRAE standard 55-2017 by the University of California at Berkeley.

Numerical simulation

Three-dimensional models of the room are created using ANSYS Discovery SpaceClaim. For the airflow analysis, a larger domain was created outside the case considered. The size and extent of the outer domain were calculated (Figure 1 (b) as recommended by Franke et al. (2004), and a domain of 63.4m × 34.3m × 18m was created. Tetrahedral meshing is implemented to perform the numerical study. It was assumed that the airflow is by wind only and the two windows, and door considered are the only way for air exchange into and out of the space.

A wind velocity of 3m/s measured by a local weather station installed on the site at a height of 12m from ground is considered as the inlet boundary condition of the larger outer domain. The outdoor air temperature is specified as 307K whereas the surface temperatures for the floor, sidewalls and roof are considered as 305K, 306K and 308K respectively as per the measurements conducted on a summer afternoon with an infrared thermometer. Heat flux conditions of 400 kW/m^2 and 400 W/m^2 were applied for the flame of the stove and refrigerator, respectively. Room walls were given a no-slip boundary condition. A summary of the boundary conditions applied is given in Table 2.

TABLE 2. Boundary Conditions.

Boundary	Conditions
Inlet	Velocity–3m/s, Temperature–307K
Outlet	Relative Pressure–101325 Pa
Wall	No-slip wall, Temperature–306K
Ceiling	No-slip wall, Temperature–308K
Floor	No-slip wall, Temperature–305K
Refrigerator	Heat Flux–400W/m^2
Stove flame	Heat Flux–400000W/m^2

TABLE 3. Number of nodes in the grid sensitivity analysis.

Case	Without insect-proof screen	With insect-proof screen
Coarse grid	31,985	46,494
Basic grid	70,682	2,75,833
Fine grid	1,24,013	4,01,490

The insect-proof screen is simulated as a porous medium of porosity 0.9. The screen permeability and inertial factor for the screen are calculated by equation (11). Age of the air was estimated using the transport equation in the fluid model. Turbulence is modelled by the standard k-ε model. Double precision segregated solver in Fluent 19.2 is used to solve the flow domain. The second-order upwind scheme is adopted for discretising the convection schemes, and a convergence criterion of 10^{-4} is chosen for all equations except the energy equation, which is 10^{-6}.

A grid sensitivity analysis has been conducted initially to establish the independence of results with the chosen grid structure. Three grids which are coarse, basic and fine are subjected to the analysis for the cases with and without an insect-proof screen as given in Table 3.

The values of velocity and mean age of air at a line in the middle of the room in the X-direction at a level of 1.10m from the ground level are plotted for comparison in the grid sensitivity analysis as shown in Figure 2. It is evident that the results obtained with basic and fine mesh structures do not vary much, whereas the results from the coarse mesh structure varied significantly from the other two.

Hence, for optimizing the accuracy as well as the computational time required for the analysis, the basic mesh structure was adopted for the study case. The final model has the global number of nodes as 70,682 in the case without insect-proof screen and 2,75,833 in the case with insect-proof screen.

Experimental validation

Experimental measurements were conducted in the kitchen with insect proof screens on the windows with properties similar to the boundary conditions mentioned for the numerical simulation to validate the air velocity and air temperature predicted by the simulations. The air velocity was measured using the instrument HD32.3 designed for measuring microclimate manufactured by DELTA OHM. The probes for measurement include HP3217.2R (combined probe for temperature and relative humidity with accuracy of class 1/3 DIN for temperature and ±1.5% for RH), TP3276.2 (globe thermometer probe with accuracy of class 1/3 DIN) and AP3203.2 (probe with hot omnidirectional wire for air velocity with accuracy of ±0.2 m/s). The calibration of each probe has been conducted in DELTA OHM metrology laboratories.

The instruments were mounted as a tree at three levels—0.1m, 1.1m and 1.7m from the floor level. The levels were adapted from the ASHRAE standard 55: 2013 for evaluating the comfort of standing occupants as most of the kitchen work is carried out in standing position. The measurement was conducted in grid points at a spacing of 0.60cm by moving the anemometer tree at an interval of 5 minutes. Measurements were taken at 48 points, which consists of 16 points each at 0.1m, 1.1m and 1.7m level from the floor plane (Figure 3). The simulated and measured values of air velocity in each case are plotted in Figure 4.

FIGURE 2. (a) Velocity (m/s) without insect-proof screen (b) Age of Air (s) without insect-proof screen (c) Velocity (m/s) with insect-proof screen (d) Age of Air (s) with insect-proof screen.

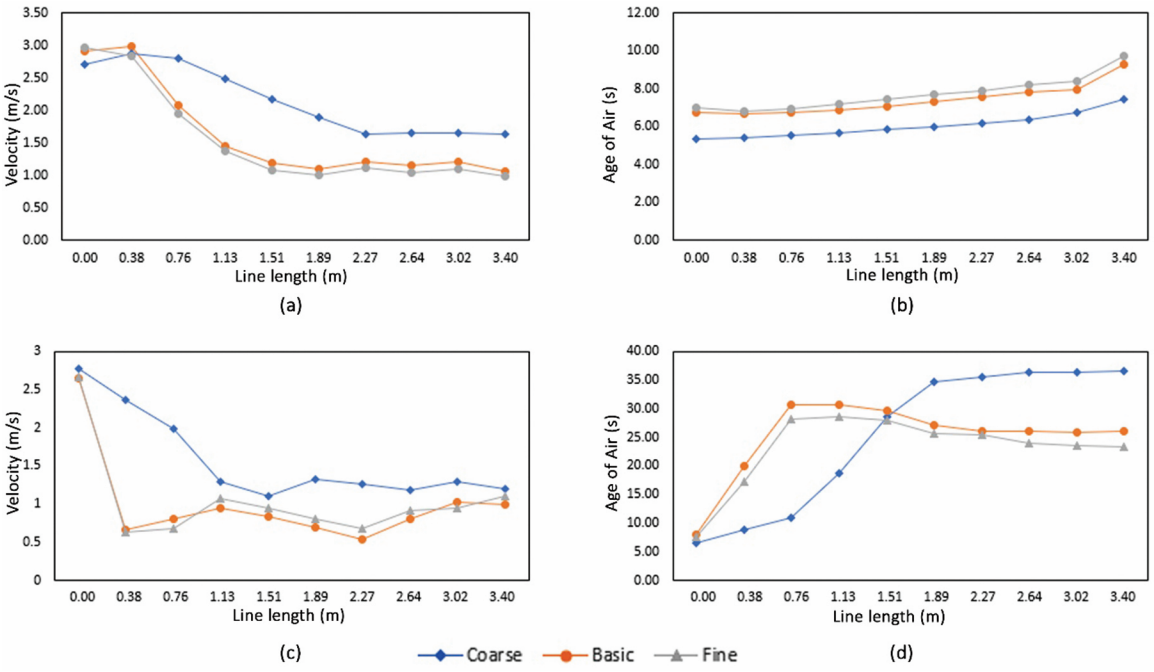

FIGURE 3. (a) Grid points where the measurements were taken. (b)Instrument set-up.

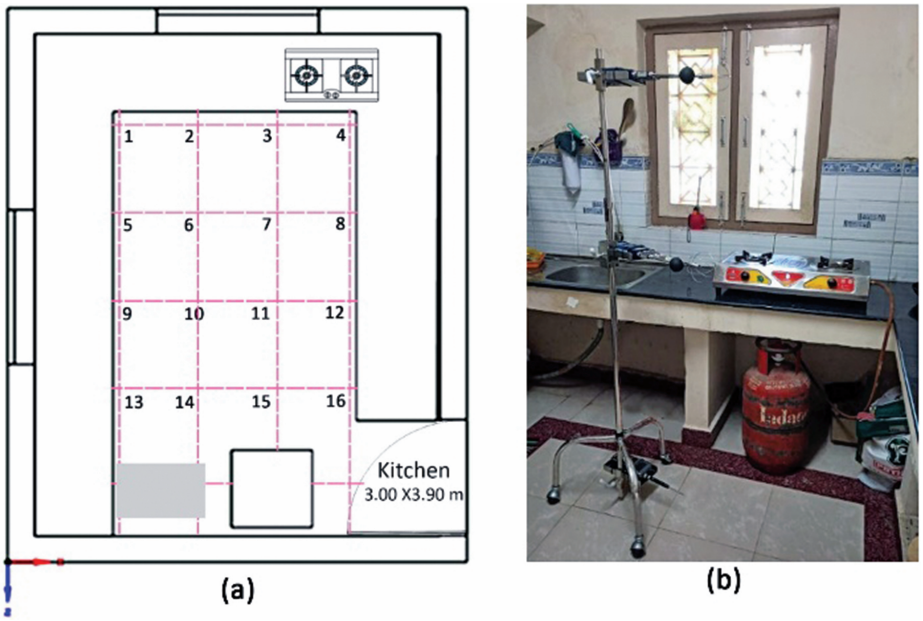

FIGURE 4. Simulated and measured values of air velocity at 16 sample points of (a) 0.1m (b)1.1m (c)1.7m without insect-proof screen and (d) 0.1m (e)1.1m (f)1.7m with insect-proof screen.

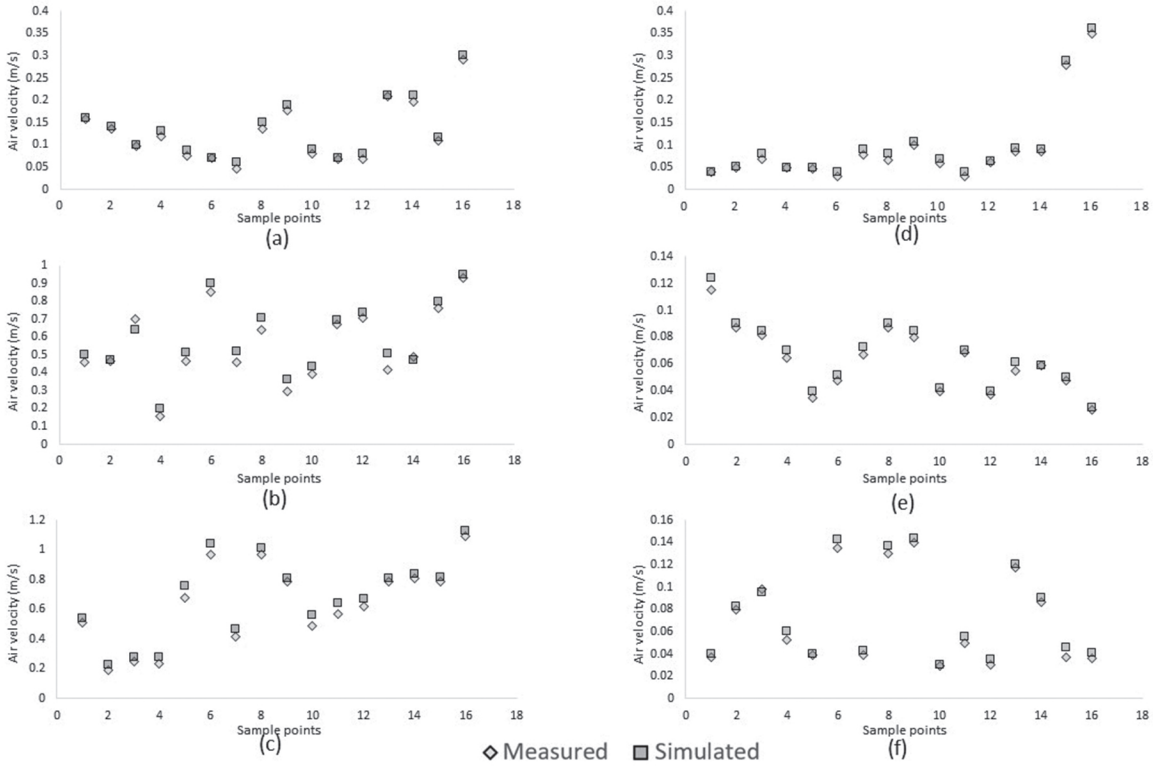

Measured values and simulated results at the considered points are compared to assess the percentage of error in each plane in both cases as given in Table 4. The average error in each case is calculated and given in Table 4. The simulated values are observed to be slightly higher than the measurement values for both temperature and air velocity. The variation in the measured and simulated values can be due to the difference domain considerations. An empty domain was considered in the simulation; however, the actual scenario with trees and other obstructions affects the airflow into the buildings. An error percentage of less than 10% is considered as a good agreement between the measured and simulated values for airflow and turbulence in enclosed environments (Z. Zhang et al., 2011).

TABLE 4. Percentage of error between the simulated and measured values.

Case	Air velocity			Air Temperature		
	0.1m level	1.1m level	1.7m level	0.1m level	1.1m level	1.7m level
Without insect-proof screen	6.19%	5.95%	6.48%	2.67%	2.70%	2.57%
With insect-proof screen	6.55%	5.62%	5.45%	2.71%	2.73%	2.64%

RESULTS AND DISCUSSIONS

The velocity, Age of Air and Temperature predicted by the numerical simulation was plotted on a plane on 3 levels—0.1m, 1.1m and 1.7m along the Y-axis. The Air Change Effectiveness (ACE) is assessed at 1.10m from the floor level for the cases with and without the insect-proof screen. The details of each parameter considered are discussed in the following sections.

Velocity

This section gives an overview of the variation in velocity with the presence and absence of insect-proof screens at the above-mentioned levels, as shown in Figure 5 and Figure 6. The air enters the space through open windows and flows outwards through the open door. For the considered air velocity of 3 m/s at the outer domain, the air velocity through the window with and without an insect-proof screen is 0.35 m/s and 1.92 m/s respectively at the level of 1.7m from floor level. The same approach to measuring yields 0.26 and 1.53m/s at 1.1m from the floor. This shows a reduction of 82% in the air velocity due to the presence of an insect-proof screen. However, the air distribution inside the space becomes almost uniform when an insect-proof screen is introduced. The recirculation of air increased the air temperature, which is discussed in the following section.

FIGURE 5. Velocity (m/s) at (a)0.1m, (b)1.1m and (c)1.7m without insect-proof screen.

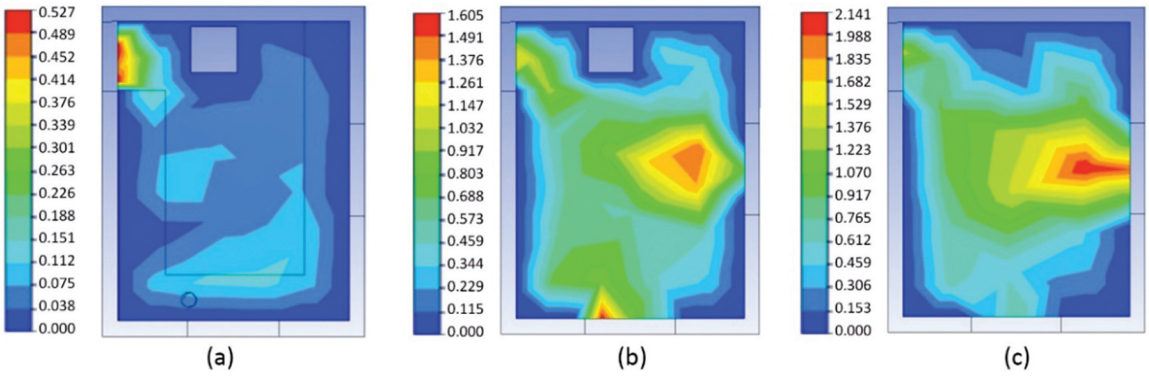

FIGURE 6. Velocity (m/s) at (a)0.1m, (b)1.1m and (c)1.7m with insect-proof screen.

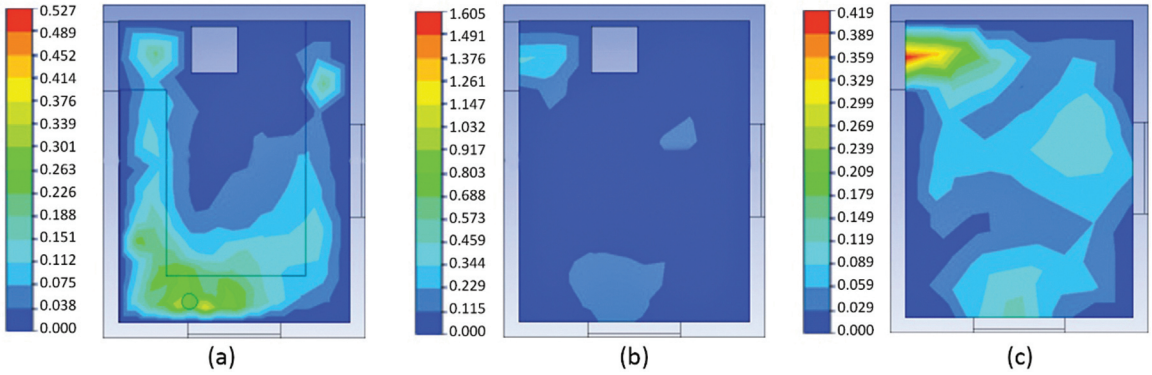

Temperature

The temperature of the air is uniformly distributed in both cases, as shown in Figure 7 and Figure 8. The only source of high temperature is restricted to the area where the flame of the gas stove and backside of the refrigerator are modelled. However, in the case with the insect-proof screen, the high temperature near the flame is spread over the space, as seen in Figure 8, creating a high-temperature zone. These high-temperature pockets can be attributed to the lower air velocity of air movement, as discussed earlier. The temperature inside the space at a level of 1.70m from the floor level (i.e., at the head height) is found to be 1K higher with the presence of an insect-proof screen.

Mean Age of Air (MAA)

The age of air varied from 0 to 35 seconds when the window is not installed with insect-proof screens (Figure 9). But, with the installation of the insect-proof screen on windows, the age of air was increased to 249 seconds (Figure 10). In the first case, the highest age of air (35 seconds) was concentrated on a corner of the space. Whereas, in the second case, more than 75% area of the space is occupied by air having age more than 103 seconds. This indicates a considerable increase in the age of air which can be approximated as a 7-fold increase when the insect-proof screen is introduced. The higher age of air is an implication of the reduced efficiency in ventilation with the presence of old air which needs to be replaced with fresh air.

FIGURE 7. Temperature (K) at (a)0.1m, (b)1.1m and (c)1.7m without insect-proof screen.

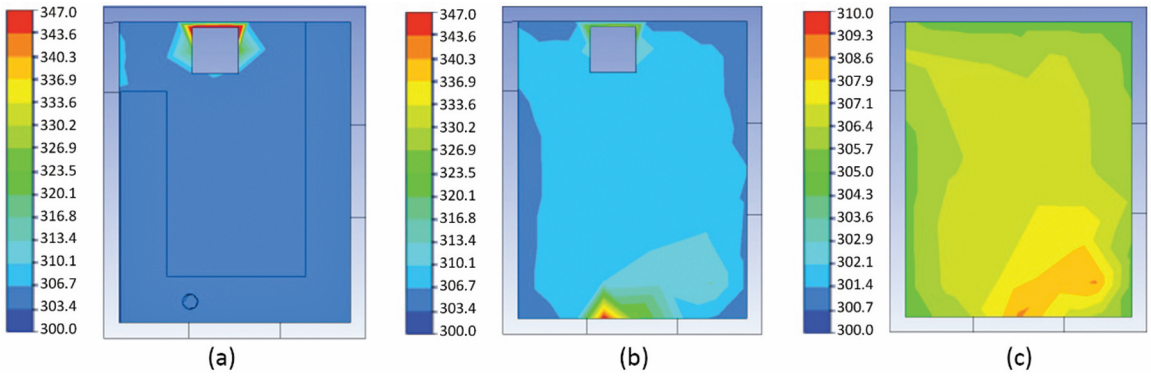

FIGURE 8. Temperature (K) at (a)0.1m, (b)1.1m and (c)1.7m with insect-proof screen.

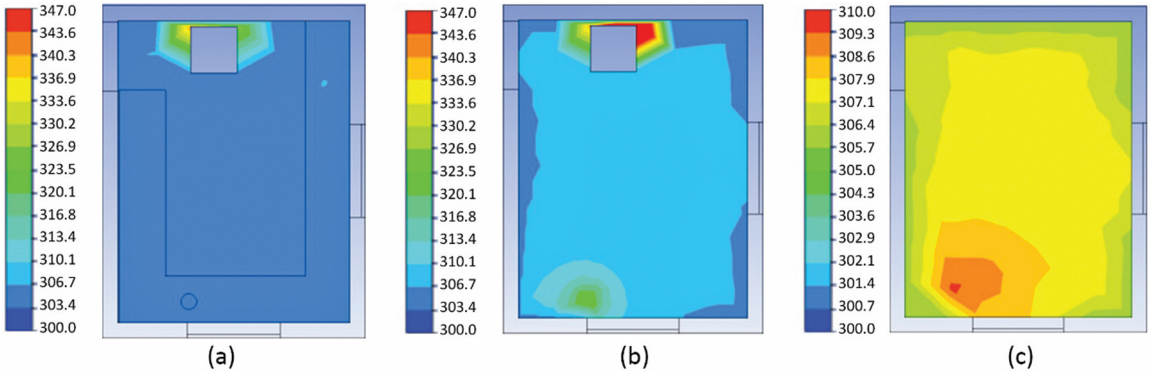

FIGURE 9. Age of Air (s) at (a) 0.1m, (b) 1.1m and (c) 1.7m without insect-proof screen.

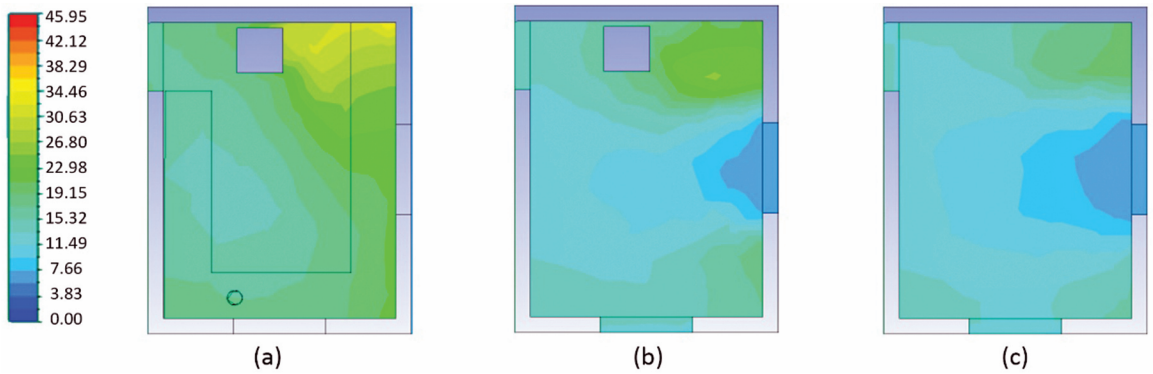

FIGURE 10. Age of Air (s) at (a) 0.1m, (b) 1.1m and (c) 1.7m with insect-proof screen.

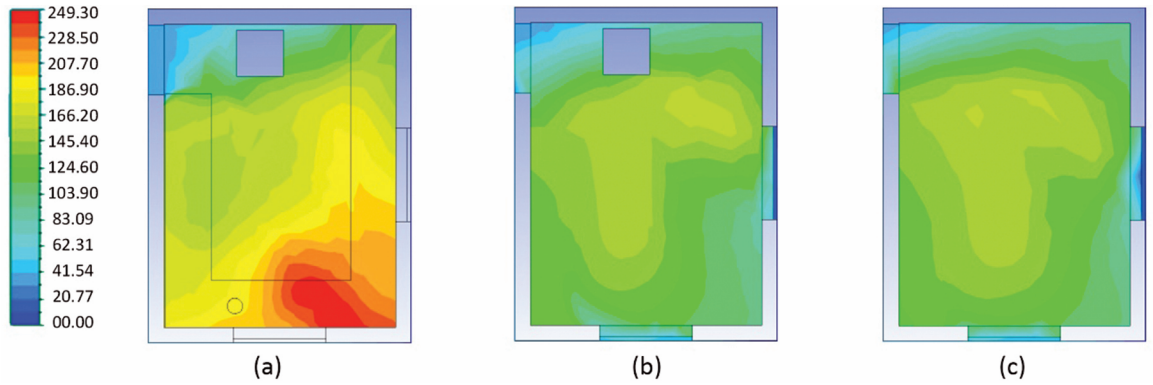

Air Change Effectiveness (ACE)

The local Air Change Effectiveness values are calculated with equations (13) and (14) at the level of 1.10m from the floor level. The ACE of the case without insect-proof screen ranges from 0.9 to 1.2; the same ranges in the second case from 0.17 to 0.33 are shown in Figure 11.

ACE indicates how well the air is distributed in a space within the breathable height. A significant decreased value of ACE also shows the poor quality of ventilation in the space under the given conditions. The presence of an insect-proof screen reduced the ACE by a factor of 70%, which will affect the thermal environment as well as the indoor air quality adversely.

Thermal comfort

Thermal comfort was assessed by coding PMV equations (Equations 15–19) as a User Defined Function (UDF) in Fluent by incorporating the elevated air speed method proposed in ASHRAE standard 55-2017 for calculating PMV when airspeed is greater than 0.1 m/s. The UDF was validated by comparing the PMV predictions with the PMV values predicted by the CBE Thermal comfort tool, which was developed according to ASHRAE standard 55-2017 by the University of California at Berkeley. The tool calculates the PMV criteria based on an elevated air speed model when the airspeed is higher than 0.2 m/s. This method considers the cooling effect provided by higher air movement. The user inputs of clothing and metabolic activity

FIGURE 11. ACE at 1.10m level (a) Without insect proof screen and (b) With insect-proof screen.

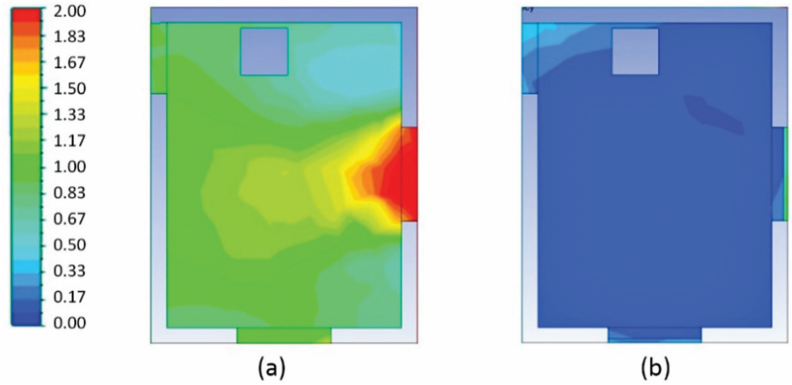

specified in the UDF along with the air velocity and air temperature predicted in Fluent are provided as inputs for the tool.

Twelve sample points along a straight line at 1.10m height in the centre of the space were chosen to compare the PMV predicted by the Fluent with the coded UDF and with the PMV predictions by the CBE thermal comfort tool as shown in Figure 12. The predictions are found to be accurate as both calculations are based on the comfort equations. Further, contour plots of the PMV predictions from the Fluent are plotted at the height of 1.10m from the floor level as given in Figure 13. Even though the temperature difference between the case with and without an insect-proof screen is only 1K approximately, the comfort votes vary largely due to the unavailability of adequate air movement in the case with insect-proof screens. The PMV was a maximum of 2.79 in the seven-point thermal sensation scale given in Table 1 which

FIGURE 12. Comparison of PMV prediction by Fluent and CBE Thermal comfort tool.

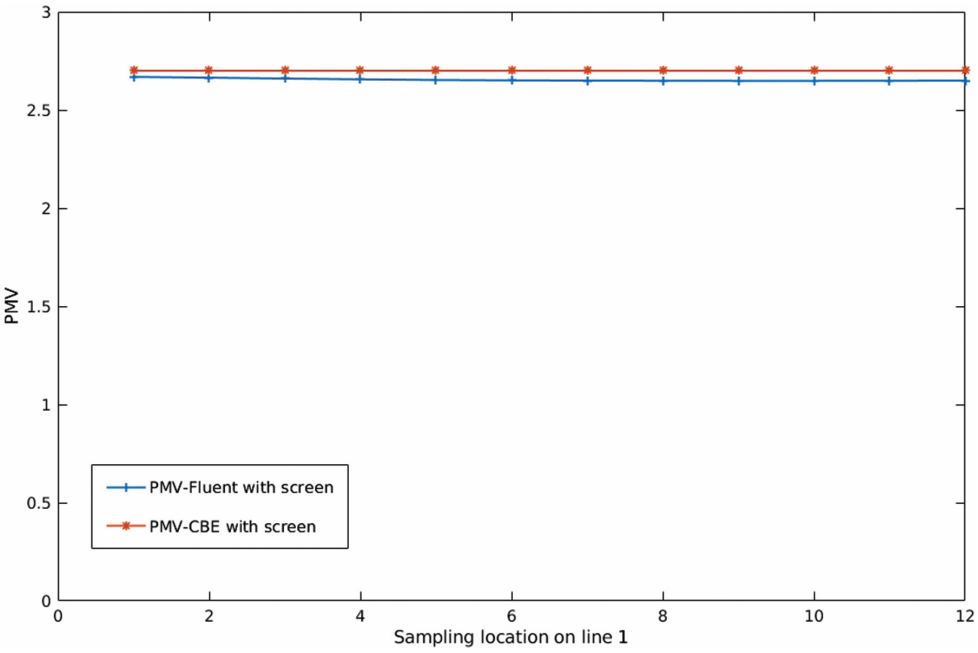

FIGURE 13. PMV at 1.10m level (a) Without insect proof screen and (b) With insect-proof screen.

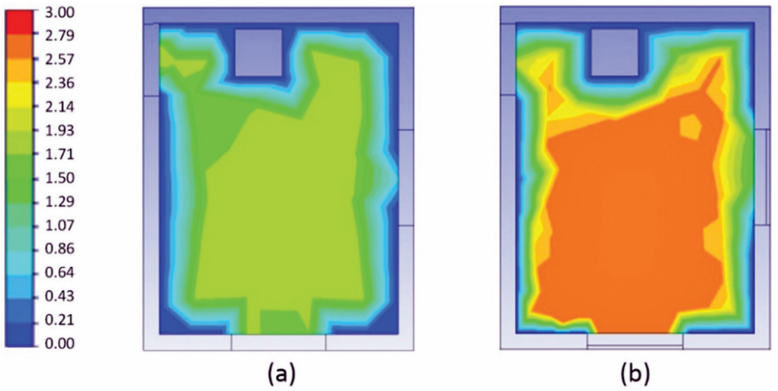

corresponds approximately to 'hot' sensation with the presence of insect-proof screens whereas, the PMV votes predicted in the case without insect-proof screens ranged up to 1.93 only which indicates a 'warm' thermal sensation only.

The results indicate that the presence of an insect-proof screen affects the thermal comfort conditions inside the space by the reduction in air velocity, air change effectiveness and increase in air temperature compared to the case without an insect-proof screen. The reported results about the presence of an insect-proof screen considerably reducing the air velocity inside the space are agreeable with the previously conducted studies (Bartzanas et al., 2002; Ravikumar & Prakash, 2011; Santolini et al., 2019). However, the variation in numerical values may be attributed to the difference in characteristics of the spaces considered in each case. The air velocity was reduced by 82–83%, which in turn increased the mean age of air inside the space, indicating the reduced efficiency in ventilation. The PMV values found in the current study has been validated with the CBE thermal comfort tool and also predicts similar results as in the previous studies (Ravikumar & Prakash, 2011) considering a habitable space. The variation in PMV values from a similar previous study (Ravikumar & Prakash, 2011) could be due to the presence of an open door and variation in the dimensions of the room and outer domain. Higher air velocities in the case without insect-proof screens provide a cooler thermal sensation compared to the case with the insect-proof screen, and the same has been considered while predicting the PMV with the elevated air speed method in ASHRAE standard 55-2013.

The reduction in Air Change Effectiveness (ACE) which resulted in warmer thermal sensation is expected to increase the energy consumption rate in the space by causing a need for alternative, active ventilation strategies that improve comfort and air quality. PMV votes were observed to be lesser in the case without insect-proof screens, i.e., where the air movement is also less. These results are agreeable with previous research on the influence of higher air velocity on increased thermal acceptability (Cândido et al., 2011). Even though there is a considerable reduction in the air velocity, the air distribution is more uniform with the presence of insect-proof screens as concluded for the case of greenhouses (Santolini et al., 2019). It should be noted that research regarding the flow through insect-proof screens are generally focused on greenhouses and crop efficiency. Further research on the effect of insect-proof screens on the thermal environment in a habitable space is required that create a better understanding on how to achieve sustainable built spaces with natural ventilation. Also, the domain considered in the

study for the boundary layer as per theoretical considerations may not be applicable in a dense urban or sub-urban scenario. The presence of other buildings, trees or any other obstructions, can alter the assumed air movement patterns; this is assumed as a major reason for variation between the simulated and measured air velocity values.

Though the insect-proof screens protect the space from insects, it results in a trade-off with the resultant thermal environment and ventilation requirements. The kitchen is a space in the residence where a higher number of air changes are required to remove contaminants generated from cooking. It is noticed that many kitchens do not have any mechanical ventilation like exhaust fans or hoods. For achieving better Indoor Air Quality (IAQ) and ventilation in residential spaces, active ventilation strategies may be adopted where the energy consumption rate will be increased. The findings highlight the need for application of a demand-controlled mechanical exhaust system as prescribed in standards(ASHRAE, 2013) that attain better Indoor Air Quality (IAQ) in kitchen spaces.

CONCLUSION

The presence of insect-proof screens on windows substantially influenced the Indoor Air Quality (IAQ) inside the kitchen in terms of reduced air velocity, increased air temperature and reduced thermal comfort and Air Change Effectiveness (ACE). The presence of an insect-proof screen reduced the air velocity inside the space by 82% compared to the case without insect-proof screens. However, the airflow pattern in the case with the screen was more uniformly distributed than the case without the screen. It is also identified that the ACE is reduced in the case with the insect-proof screen by 70%. The comfort conditions inside the space are also affected by the installation of an insect proof screen. The PMV values were increased from 1.93 to 2.79, which indicates a change from a 'warm' to 'hot' sensation with the presence of insect-proof screens. It is evident from the current study that for an efficient environment in a space with an insect-proof screen, alternative means of ventilation may be needed to ensure better air movement by reducing recirculation of air inside the room and improve thermal comfort. Alternative active ventilation strategies may lead to increased energy consumption in the space. Further research is required on the role of active ventilation mechanisms on energy and occupant comfort.

ACKNOWLEDGEMENT

This work was supported in part by the Department of Science and Technology, Ministry of Science and Technology, Government of India through the project—Community-Scale Energy Demand Reduction in India (CEDRI) under Grant DST/TMD/UK-BEE/2017/20.

REFERENCES

Al Horr, Y., Arif, M., Kaushik, A., Mazroei, A., Katafygiotou, M., & Elsarrag, E. (2016). Occupant productivity and office indoor environment quality: A review of the literature. *Building and Environment, 105*, 369–389. https://doi.org/10.1016/j.buildenv.2016.06.001

Angelopoulos, C., Cook, M. J., Iddon, C. R., & Porritt, S. M. (2017). Evaluation of thermal comfort in naturally ventilated school classrooms using CFD. *15th Conference of International Building Performance Simulation Association*.

ASHRAE, A. (2013). *ANSI/ASHRAE Standard 62.2-2013. Ventilation and Acceptable Indoor Air Quality in Low-Rise Residential Buildings*.

Bartzanas, T., Kittas, C., & Boulard, T. (2002). Numerical simulation of the airflow and temperature patterns in a greenhouse equipped with insect-proof screen in the openings. *Acta Horticulturae, 578*, 351–358. https://doi.org/10.1016/S0168-1699(01)00188-0

Cândido, C., de Dear, R. J., Lamberts, R., & Bittencourt, L. (2010). Air movement acceptability limits and thermal comfort in Brazil's hot humid climate zone. *Building and Environment, 45*(1), 222–229. https://doi.org/10.1016/j.buildenv.2009.06.005

Cândido, C., de Dear, R., & Lamberts, R. (2011). Combined thermal acceptability and air movement assessments in a hot humid climate. *Building and Environment, 46*(2), 379–385. https://doi.org/10.1016/j.buildenv.2010.07.032

Cehlin, M., Larsson, U., & Chen, H. J. (2018). Numerical Investigation of Air Change Effectiveness in an Office Room with Impinging Jet Ventilation. *4th International Conference On Building Energy, Environment*, 641–646.

Chen, Z., Xin, J., & Liu, P. (2020). Air quality and thermal comfort analysis of kitchen environment with CFD simulation and experimental calibration. *Building and Environment*, 106691. https://doi.org/10.1016/j.buildenv.2020.106691

Cohen, M. (2015). *Modelling of Airflow through Wire Mesh Security Screens*. https://ojs.unsw.adfa.edu.au/index.php/juer/article/view/920/557

Debnath, R., Bardhan, R., & Banerjee, R. (2016a). Evaluating Differences in Airflow Patterns For Similar Rural Kitchens Using CFD. *Sixth International Congress on Computational Mechanics and Simulation (ICCMS-2016), 27 June–1 July, 2016*, 390–394. http://www.iccms2016.org/Docs/ICCMS_Proceeding.pdf

Debnath, R., Bardhan, R., & Banerjee, R. (2016b). Investigating the age of air in rural Indian kitchens for sustainable built-environment design. *Journal of Building Engineering, 7*, 320–333. https://doi.org/10.1016/j.jobe.2016.07.011

Fanger, P. O. (1970). Thermal comfort. Analysis and applications in environmental engineering. *Thermal Comfort. Analysis and Applications in Environmental Engineering*.

Fatnassi, H., Boulard, T., Poncet, C., & Chave, M. (2006). Optimisation of greenhouse insect screening with computational fluid dynamics. *Biosystems Engineering, 93*(3), 301–312. https://doi.org/10.1016/j.biosystemseng.2005.11.014

Feriadi, H., & Wong, N. H. (2004). Thermal comfort for naturally ventilated houses in Indonesia. *Energy and Buildings, 36*(7), 614–626. https://doi.org/10.1016/j.enbuild.2004.01.011

Franke, J., Hirsch, C., Jensen, A. G., Krus, H. W., Schatzmann, M., Miles, P. S. W. and S. D., Wisse, J. A., & Wright, N. G. (2004). Recommendations on the Use of CFD in Wind Engineering. *Cost Action C, 14*(January), C1.

Ge, Z., Xu, G., Poh, H. J., Ooi, C. C., & Xing, X. (2019). CFD simulations of thermal comfort for naturally ventilated school buildings. *IOP Conference Series: Earth and Environmental Science, 238*(1). https://doi.org/10.1088/1755-1315/238/1/012073

Haase, M., & Amato, A. (2009). An investigation of the potential for natural ventilation and building orientation to achieve thermal comfort in warm and humid climates. *Solar Energy, 83*(3), 389–399. https://doi.org/10.1016/j.solener.2008.08.015

Hawendi, S., Gao, S., & Ahmed, A. Q. (2019). Effect of heat loads and furniture on the thermal comfort of an isolated family house under a naturally ventilated environment. *International Journal of Ventilation, 0*(0), 1–26. https://doi.org/10.1080/14733315.2019.1600815

Hellström, J. G. I., & Lundström, T. S. (2006). Flow through Porous Media at Moderate Reynolds Number. *International Scientific Colloquium—Modelling for Material Processing*, 129–134.

Horikiri, K., Yao, Y., & Yao, J. (2014). Modelling conjugate flow and heat transfer in a ventilated room for indoor thermal comfort assessment. *Building and Environment, 77*, 135–147. https://doi.org/10.1016/j.buildenv.2014.03.027

Horikiri, K., Yao, Y., & Yao, J. (2015). Numerical optimisation of thermal comfort improvement for indoor environment with occupants and furniture. *Energy and Buildings, 88*, 303–315. https://doi.org/10.1016/j.enbuild.2014.12.015

Hormigos-Jimenez, S., Padilla-Marcos, M. Á., Meiss, A., Gonzalez-Lezcano, R. A., & Feijó-Muñoz, J. (2018). Computational fluid dynamics evaluation of the furniture arrangement for ventilation efficiency. *Building Services Engineering Research and Technology, 39*(5), 557–571. https://doi.org/10.1177/0143624418759783

Indraganti, M. (2010). Behavioural adaptation and the use of environmental controls in summer for thermal comfort in apartments in India. *Energy and Buildings, 42*(7), 1019–1025. https://doi.org/10.1016/j.enbuild.2010.01.014

Karacavus, B., & Aydin, K. (2018). Numerical investigation of general and local thermal comfort of an office equipped with radiant panels. *Indoor and Built Environment, 28*(6), 806–824. https://doi.org/10.1177/1420326X18799834

Kwok, Y. T., Lau, K. K. L., Lung Lai, A. K., Chan, P. W., Lavafpour, Y., Kwan Ho, J. C., & Yung Ng, E. Y. (2017). A comparative study on the indoor thermal comfort and energy consumption of typical public rental housing types under near-extreme summer conditions in Hong Kong. *Energy Procedia, 122*, 973–978. https://doi.org/10.1016/j.egypro.2017.07.454

López, A., Molina-Aiz, F. D., Valera, D. L., & Peña, A. (2016). Wind tunnel analysis of the airflow through insect-proof screens and comparison of their effect when installed in a mediterranean greenhouse. *Sensors (Switzerland), 16*(5), 5–8. https://doi.org/10.3390/s16050690

Loveday, D., Webb, L., Verma, P., Cook, M. J., Rawal, R., Vadodaria, K., Cropper, P., Brager, G. S., Zhang, H., Foldvary, V., Arens, E., Babich, F., Cobb, R., Ariffin, R., Kaam, S., & Toledo, L. (2016). The Role of Air Motion for Providing Thermal Comfort in Residential / Mixed Mode Buildings : a Multi-partner Global Innovation Initiative (GII) Project. *Proceedings of 9th Windsor Conference: Making Comfort Relevant, April*, 947–962.

Manu, S., Shukla, Y., Rawal, R., Thomas, L. E., de Dear, R., Dave, M., & Vakharia, M. (2014). Assessment of Air Velocity Preferences and Satisfaction for Naturally Ventilated Office Buildings in India. *PLEA 2014: 30th Conference on Passive and Low Energy Architecture, December*, 1–8.

Miguel, A. F. (1998). Airflow through porous screens: From theory to practical considerations. *Energy and Buildings, 28*(1), 63–69. https://doi.org/10.1016/S0378-7788(97)00065-0

Miguel, A. F., Van De Braak, N. J., & Bot, G. P. A. (1997). Analysis of the airflow characteristics of greenhouse screening materials. *Journal of Agricultural and Engineering Research, 67*(2), 105–112. https://doi.org/10.1006/jaer.1997.0157

Muñoz, P., Montero, J. I., Antón, A., & Giuffrida, F. (1999). Effect of insect-proof screens and roof openings on greenhouse ventilation. *Journal of Agricultural and Engineering Research, 73*(2), 171–178. https://doi.org/10.1006/jaer.1998.0404

Nielsen, P. V. (2015). Fifty years of CFD for room air distribution. *Building and Environment, 91*, 78–90. https://doi.org/10.1016/j.buildenv.2015.02.035

Norris, N., & Collins, M. (2008). *Modelling the effects of insect screens on natural convection in Window Cavities* (pp. 1–9).

Persily, A. (2015). Challenges in developing ventilation and indoor air quality standards: The story of ASHRAE Standard 62. *Building and Environment, 91*, 61–69. https://doi.org/10.1016/j.buildenv.2015.02.026

Ravikumar, P., & Prakash, D. (2011). Analysis of thermal comfort in a residential room with insect proof screen: A case study by numerical simulation methods. *Building Simulation, 4*(3), 217–225. https://doi.org/10.1007/s12273-011-0032-9

Ravindra, K., Agarwal, N., Kaur-sidhu, M., & Mor, S. (2019). Appraisal of thermal comfort in rural household kitchens of Punjab, India and adaptation strategies for better health. *Environment International, 124*(December 2018), 431–440. https://doi.org/10.1016/j.envint.2018.12.059

Sabie, D. D., & Ghiaus, A.-G. (2019). Influence of furniture arrangement on airflow distribution in open concept passive houses. *E3S Web of Conferences, 85*, 01010. https://doi.org/10.1051/e3sconf/20198501010

Santolini, E., Pulvirenti, B., Torreggiani, D., & Tassinari, P. (2019). Novel methodologies for the characterization of air flow properties of shading screens by means of wind-tunnel experiments and CFD numerical modeling. *Computers and Electronics in Agriculture, 163*(April), 104800. https://doi.org/10.1016/j.compag.2019.05.009

Sarkar, A., & Bardhan, R. (2018). Optimizing Interior Layout for Effective Experiential Indoor Environmental Quality in Low-income Tenement Unit: A Case of Mumbai, India. *Building Simulation & Optimization Conference, September*, 11–12.

Snehalatha, K. S., Ramaiah, K. D., Vijay Kumar, K. N., & Das, P. K. (2003). The mosquito problem and type and costs of personal protection measures used in rural and urban communities in Pondicherry region, South India. *Acta Tropica, 88*(1), 3–9. https://doi.org/10.1016/S0001-706X(03)00155-4

Tarantini, M., Pernigotto, G., & Gasparella, A. (2017). A co-citation analysis on thermal comfort and productivity aspects in production and office buildings. *Buildings, 7*(2). https://doi.org/10.3390/buildings7020036

Teitel, M. (2010). Using computational fluid dynamics simulations to determine pressure drops on woven screens. *Biosystems Engineering, 105*(2), 172–179. https://doi.org/10.1016/j.biosystemseng.2009.10.005

Tong, Z., Chen, Y., Malkawi, A., Liu, Z., & Freeman, R. B. (2016). Energy saving potential of natural ventilation in China: The impact of ambient air pollution. *Applied Energy, 179*, 660–668. https://doi.org/10.1016/j.apenergy.2016.07.019

Valera, D. L., Álvarez, A. J., & Molina, F. D. (2006). Aerodynamic analysis of several insect-proof screens used in greenhouses. *Spanish Journal of Agricultural Research, 4*(4), 273–279. https://doi.org/10.5424/sjar/2006044-204

Valera, D. L., Molina, F. D., Álvarez, A. J., López, J. A., Terrés-Nicoli, J. M., & Madueño, A. (2005). Contribution to characterisation of insect-proof screens: Experimental measurements in wind tunnel and CFD simulation. *Acta Horticulturae, 691*(February 2015), 441–448.

Vijayalaxmi, J., & Sekar, S. (2010). Indoor Thermal Performance of Ventilated Dwellings Using Fly Screens in the Hot-Humid Climate of Chennai, India. *Journal of Green Building, 4*(2), 150–157. https://doi.org/10.3992/jgb.4.2.150

Wong, N. H., Feriadi, H., Lim, P. Y., Tham, K. W., Sekhar, C., & Cheong, K. W. (2002). Thermal comfort evaluation of naturally ventilated public housing in Singapore. *Building and Environment, 37*(12), 1267–1277. https://doi.org/10.1016/S0360-1323(01)00103-2

Zhang, Q., & Yu Lau, S. S. (2017). Let in the wind: A passive design paradigm for large buildings in the Inner city of Shanghai and Singapore. *WIT Transactions on Ecology and the Environment, 223*, 215–225. https://doi.org/10.2495/SC170191

Zhang, Z., Zhang, W., Zhai, Z. J., Chen, Q. Y., Zhai, Z. J., & Chen, Q. Y. (2011). Evaluation of Various Turbulence Models in Predicting Airflow and Turbulence in Enclosed Environments by CFD: Part 2—Comparison with Experimental Data from Literature Evaluation of Various Turbulence Models in Predicting Airflow and Turbulence in Enclo. *HVAC&R Research, 9669*(February 2016), 37–41. https://doi.org/10.1080/10789669.2007.10391460